COMPUTED STRUCTURE OF NEAR-COHERENT TWIN BOUNDARIES COMPARED WITH TEM OBSERVATIONS

DEHOSSON, JTM; SCHAPINK, FW; HERINGA, [No Value]; HAMELINK, JJC

Published in:
Acta Metallurgica

DOI:
10.1016/0001-6160(86)90215-4

Acta metall. Vol. 34, No. 6, pp. 1051–1057, 1986
Printed in Great Britain.

0001-6160/86 $3.00 + 0.00

COMPUTED STRUCTURE OF NEAR-COHERENT TWIN BOUNDARIES COMPARED WITH TEM OBSERVATIONS

J. TH. M. DE HOSSON,[1] F. W. SCHAPINK,[2] J. R. HERINGA[1] and J. J. C. HAMELINK[2]

[1]Department of Applied Physics, Materials Science Centre, University of Groningen, Nijenborgh 18, 9747 AG Groningen, The Netherlands and [2]Laboratory of Metallurgy, Delft University of Technology, Rotterdamseweg 137, 2628 AL Delft, The Netherlands

(*Received* 5 *July* 1985; *in revised form* 10 *September* 1985)

Abstract—The structure of a near-coherent twin boundary in a Au bicrystal was investigated using transmission electron microscopy. Upon annealing the bicrystal, a low angle boundary and a parallel coherent twin boundary merged to form a near-coherent twin boundary with a deviation of 0.45° from the exact twin orientation. In the near-coherent twin boundary a dislocation network has been observed with a characteristic six-star pattern, while in some small areas the network has a triangular shape which is closely related to the six-star pattern. In an effort to reproduce these patterns in a computer simulation study, the atomic configurations in (111) twist boundaries close to the twin orientation were calculated (Σ37, Σ61, Σ91, Σ127, Σ169). For a given twist boundary and interatomic potential both six-star and triangular patterns were obtained. The triangular structure appeared to be energetically much more favourable, independent of the various interatomic potentials employed.

Résumé—Nous avons étudié par microscopie électronique en transmision la structure d'un joint de macle presque cohérent dans un bicristal d'or. Au cours d'un recuit du bicristal, un sous-joint et un joint de macle cohérent parallèle fusionnent pour former un joint de macle presque cohérent, avec une déviation de 0,45° par rapport á l'orientation de macle exacte. Dans le joint de macle presque cohérent, nous avons observé un réseau de dislocations en forme d'étoile à six branches, alors que dans d'autres régions, le réseau a une forme triangulaire qui est étroitement liée à l'étoile à six branches. Afin d'essayer de reproduire ces configurations dans une étude par simulation sur ordinateur, nous avons calculé les configurations atomiques dans des joints de torsion (111) proches de l'orientation de macle (Σ37, Σ61, Σ91, Σ127, Σ169). Pour un joint de torsion et un potentiel interatomique donnés, nous avons obtenu les configurations en étoile et en triangle. La structure triangulaire était énergétiquement beaucoup plus favorable, quels que soient les potentiels interatomiques utilisés.

Zusammenfassung—Die Struktur einer Zwillingskorngrenze in der Nähe der Kohärenz wurde in einem Au-Bikristall elektronenmikroskopisch untersucht. Nach der Auslagerung des Bikristalles reagierten eine Kleinwinkelkorngrenze und eine parallele kohärente Zwillingskorngrenze zu einer Zwillingskorngrenze nahe der Kohärenz mit einer Abweichung von 0.45° von der exakten Zwillingsorientierung. In dieser Korngrenze wurde eine Versetzungsnetzwerk beobachtet, welches ein charakteristisches sechseckiges Muster aufwies; in einigen kleinen Bereichen hat das Netzwerk eine eher dreieckige, der sechseckigen ähnlich Struktur. Um diese Strukturen in einem Computermodell zu reproduzieren, wurden die Atomkonfigurationen in (111) Drill-Korngrenzen in der Nähe der Zwillingsorientierung berechnet (Σ37, Σ61, Σ91, Σ127, Σ169). Für eine gegebene Drill-Korngrenze und ein gegebenes interatomares Potential wurden sowohl sechs- als auch dreieckige Muster erhalten. Die dreieckige Anordnung ist energetisch viel stabiler, unabhängig vom benutzten interatomaren Potential.

1. INTRODUCTION

In contrast to dislocations, grain boundaries do not possess a long range stress field. As a consequence, their effects on materials behaviour are determined by their local atomic configurations. Over the past decades, these local atomic configurations have been investigated with increasing frequency, using computer simulation techniques. Since important aspects of grain boundary behaviour are complex phenomena, which tend to be resistant to analytical treatment, computer simulations have become very useful in understanding some of the basic concepts. For a review reference is made to [1, 2].

Comparing the computational results with experimental data is often a difficult task because the core regions of grain boundaries cannot reliably be investigated experimentally. In the present investigation, this problem is solved by carrying the detailed atomic calculation of grain boundary structures to the point where they qualitatively reveal the observed structures.

Direct motivation for a computer simulation study stems from the experimental investigation of the structure in (111) Au bicrystals using transmission electron microscopy. In particular, the *in situ* annealing of a bicrystal, containing a low angle twist boundary and at least one coherent twin boundary was studied by TEM (Section 2). The coalescence of these boundaries led predominantly to the formation of characteristic six-star dislocation networks consisting of three parallel sets of Shockley partial dislocations with associated steps in the twin boundary.

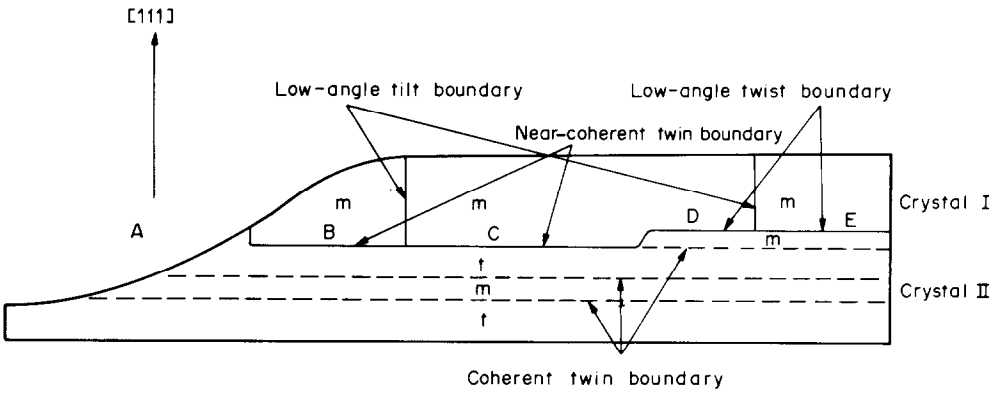

Fig. 1. Schematic side view of the specimen, showing the various grain boundaries present.

It suggests that the most stable atomic configuration is a micro-faceted configuration. So far, faceting has mainly been studied in tilt boundaries [3, 4]. In an effort to reproduce the observed six-star patterns, the atomic configurations in (111) twist boundaries close to the twin misorientation were calculated. The computational results are described in Section 3 and discussed in Section 4 in comparison with experiments.

2. TEM OBSERVATIONS

The Au bicrystals used in this investigation were prepared from thin (111) Au single crytals according to the method described elsewhere [5]. In Fig. 1 schematic view of the specimen is depicted, showing the various boundaries present. Crystal I contains a number of areas, surrounded by low angle tilt boundaries. In crystal II a number of coherent twin boundaries are present parallel to the surface. Upon annealing at 475 K one of these twin boundaries, together with the original low angle twist boundary, forms a near -coherent twin boundary with a misorientation of 0.9° and 0.45° around the common [111] axis in areas B and C, respectively. Regions B and C are separated by a low-angle vertical tilt boundary accommodating the misfit difference, as discussed in more detail elsewhere [6].

In area C of the near-coherent twin boundary a dislocation network is observed which has the shape of a six-star pattern. Weak-beam images were analysed for the determination of the Burgers vectors and the exact shape of the dislocation network. The Burgers vectors are of the type 1/6 $\langle 11\bar{2}\rangle$ and the dislocation spacings are 16 nm and 32 nm for areas B and C, respectively. Figure 2 shows a dark-field micrograph of these areas taken with the matrix diffraction vector $[\bar{1}1\bar{1}]_m$. Because the orientation of the electron beam was near the $[121]_m$ axis, no corresponding twin reflection $(111)_t$ was excited and consequently no Moiré effects will complicate the image interpretation, as has been discussed by Hamelink and Schapink [7]. It is well known that a 1/6 $\langle 11\bar{2}\rangle$ dislocation in a coherent twin boundary causes a step in the boundary equal to one interplanar spacing [8]. A sequence of steps introduced by a network of $a/6\langle 11\bar{2}\rangle$ dislocations has to satisfy the condition that the average boundary normal remains equal to the [111] normal of a coherent twin boundary. Using this concept Scott and Goodhew [9] have argued that the network will take the shape of a six-star pattern, consisting of a sequence of hexagonal and triangular areas such that the triangular areas are located alternately on adjacent (111) planes above or below the plane of the hexagons. This configuration minimizes the occurrence of double steps in the boundary.

Using the matrix reflection $(\bar{1}1\bar{1})_m$ a stepped boundary configuration is imaged clearly as a black-grey-white contrast pattern (Fig. 2). At first sight, it is unexpected that these steps lead to such a strong contrast since these steps of 0.23 nm are very small relative to the extinction distance of 17 nm for a (111) reflection in Au at 120 kV. However, the presence of 1/6 $\langle 11\bar{2}\rangle$ dislocations in a near coherent twin boundary may produce a strong stacking fault-like contrast provided another parallel coherent twin boundary is present [5]. Focussed Riecke diffraction patterns confirmed that at least one coherent twin boundary is parallel to the near-coherent twin boundary. During subsequent *in situ* annealing area B in Fig. 2 was found to move, caused by the migration of the vertical tilt boundaries as explained in [6].

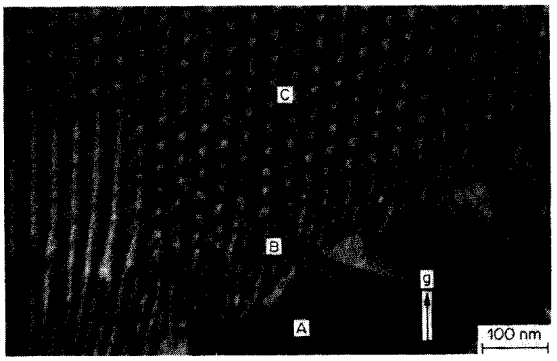

Fig. 2. Dark-field micrograph, imaged with the $(\bar{1}1\bar{1})_m$ reflection. The steps in the grain boundary caused by the network are seen as a black-grey-white contrast. The labels of several areas correspond to those in Fig. 1.

3. COMPUTATIONAL METHOD AND RESULTS

The method of calculating the "equilibrium" grain boundary structure consist essentially of a procedure for numerical integration of the equations of motion resulting from Newtonian mechanics. The first step in the simulation is the construction of a large computational block of interacting atoms. The atoms are released from an arbitrary, non-overlapping configuration within that computational block either from rest or with a random distribution of velocities. The relaxation of the individual atoms attempts to achieve a minimization of the energy of the system with respect to the positions of the atoms, assuming a suitable interatomic interaction function. The relaxation procedure employed was a static one. This type of calculation carries out the minimization of the potential enery of the atoms and corresponds to the minimization of the internal energy, E, at $T = 0$ K.

In principle one should be able to construct a realistic picture of the grainboundary structure using this method provided that the appropriate pair potential is accurately known. The accuracy of the potentials used to determine the forces between atoms is essential to the success of a computer experiment. In our study we have applied two completely different sets of potentials for Al: Lennard–Jones 6–12 potential based on the sublimation energy for aluminum [10] and a screened pseudopotential of Al (11). In the approximation of the central force, the internal energy E of a metallic system takes the form

$$E = U(\Omega_0) + 1/2 \sum_{i,j} \phi(r_{ij}, \Omega_0) \qquad (1)$$

where $U(\Omega_0)$ is a potential dependent only on the average volume per ion, Ω_0, and $\phi(r_{ij}, \Omega_0)$ is the volume-dependent pair potential acting between ions at positions $\mathbf{r}_i$ and $\mathbf{r}_j$. $U(\Omega_0)$ is structure independent and represents the average energy of the conduction electrons in the metal. It is responsible for the observed deviation from the Cauchy relation, $C_{12} = C_{44}$ in cubic metals. In quantum mechanics, expression (1) is applicable if the perturbation expansion to the second order is sufficient and the higher order terms which lead to many-body forces can be neglected, i.e. a "weak" potential as a perturbation upon a chosen ground state. A well known technique for the construction of "weak" potentials is the pseudopotential method which is, however, only applicable to simple metals. The general feature of these potentials is the long range oscillatory behaviour. The Al-potential constructed along these lines is depicted in Fig. 3. The Lennard–Jones potential, shown in Fig. 4, behaves rather differently. It represents an empirical pair potential which incorporates the volume dependent terms. At large distances, the forces fall off as the seventh power of the distance, simulating the behaviour of Van Der Waals forces between closed-shell atoms. As a result, this potential is particularly suited to describe rare gas solids, although not metals. In that sense the potential we used is rather a mathematical representation of Al than a physical description. It has to be emphasized that our atomistic study of grain boundaries is aimed at finding characteristic features of grain boundary structures, possibly depending on the mathematical form of the potential chosen, rather than at predicting structural details of grain boundary structures in Au. Since pseudopotential theory is applicable to Al, two completely different sets of potentials are available for Al, in contrast to Au.

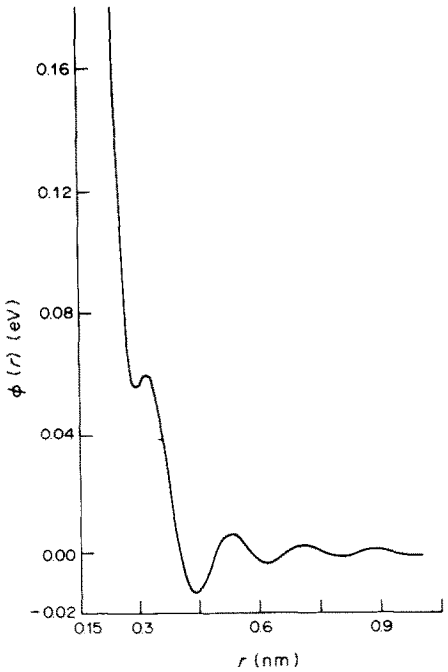

Fig. 3. Interatomic pair-potential for Al (pseudo-potential method [11].

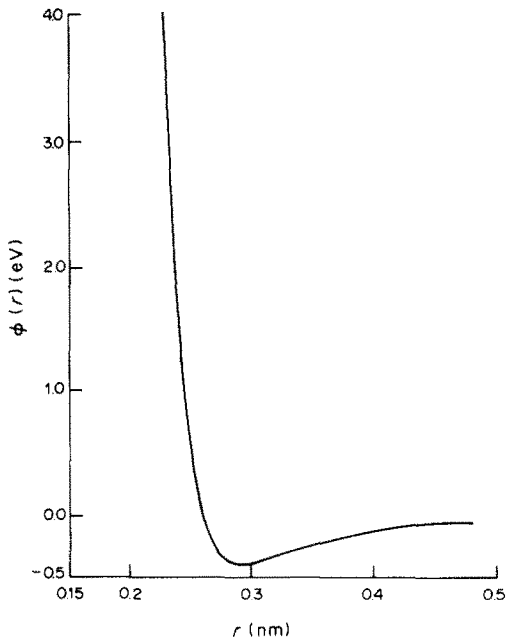

Fig. 4. L–J potential for Al [10].

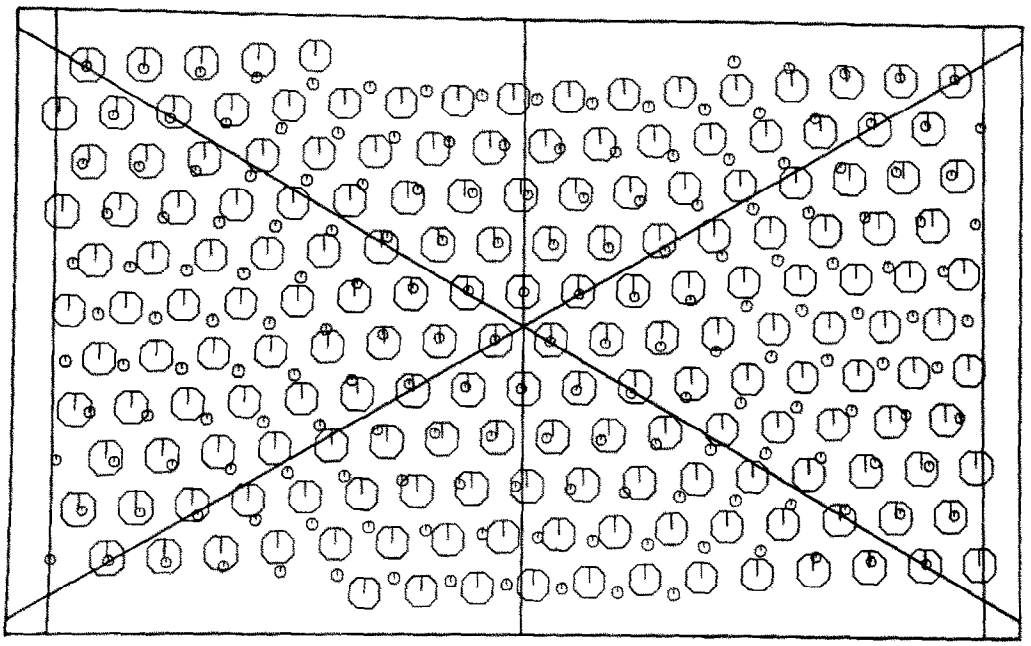

Fig. 5. Projected triangular structure of the (111) planes Z = 0 and 1 from a $\Sigma = 91$ ($\theta = 53.99°$) twist boundary.

In the computations various initial configurations were investigated. For the coincidence type boundary the original block of atoms is a geometrically constructed bicrystal corresponding to a chosen value of Σ, rotation axis and boundary plane. Σ represents the reciprocal density of coincidence sites in the unit cell of the coincidence site lattice. The atomic configurations in a number of (111) twist boundaries close to the twin orientation were calculated: $\Sigma = 37$, 50.57°; $\Sigma = 61$, 52.66°; $\Sigma = 91$, 53.99°; $\Sigma = 127$, 54.91°; $\Sigma = 169$, 55.59°. The simulated part of the crystal consists of 8 (111) lattice planes. Fixed boundary conditions were applied in the direction perpendicular to the grain boundary in the sense that on the top and bottom of the computational cell at least two extra planes were kept in their starting configuration. We have allowed for rigid translation. In directions parallel to the grain boundary, periodic boundary conditions were applied. The repeat distance was at least equal to the repeat distance of the csl cell in the boundary plane. If the starting configuration was chosen to be the exact coincidence configuration, the final atomistic structure after relaxation was found to be very similar to the initial configuration. The small differences could be demonstrated most clearly in a plot of the Fourier transform of a particular grain boundary structure [12, 13]. As a typical example, the atomic configuration of the $\Sigma = 91$ twist boundary is depicted in Fig. 5. Based upon the stacking of (111) planes, this structure can be described by a triangular network of Shockley partial dislocations, as indicated in Fig. 5. A rigid translation of one crystal with respect to the other in the starting configuration may lead to a slightly different final structure. However, in all of these configurations one finds that some atoms in the lattice planes adjacent to the boundary are at a distance closer than the nearest neighbour distance in an undistorted f.c.c. crystal. (Upto $a_0/\sqrt{3}$ vs $a_0/\sqrt{2}$ for n.n. distance in f.c.c. lattice.) Consequently these atoms produce a large contribution to the grain boundary energy due to the repulsion part in the atomic potential. In order to look for a lower energy configuration and to avoid the close approach of atom pairs in the boundary a different procedure has been adopted. To this end, the lattice plane in the middle of the computational block, has been divided in two separate sections, belonging to the upper and lower crystal, respectively, in such a way that no two atoms on different (111) planes are too close to each other in the starting configuration. The initial density of this particular plane was taken to be the same as the density of the other (111). After relaxation, structures different from those depicted in Fig. 5 were found, depending on the atomic interaction function used. Figure 6 shows that one structure obtained for $\Sigma = 91$ closely resembles the six-star pattern observed experimentally for a much smaller deviation from the twin orientation (Fig. 2). The dashed lines in Fig. 6 represent dislocation line segment lying between planes 0 and 1. The stacking sequence of (111) planes in a cross section along P_1P_3 in Fig. 6 is illustrated in Fig. 7, where the symbols I and II represent the ABC . . . and CBA . . . stacking sequence of the (111) planes. Apparently the boundary plane has a stepped character such that the double steps occur at the corners of the triangles in Fig. 6, in agreement with the experimentally observed structure of the network. There exists a close connection between the dislocation configuration of Figs 5 and 6. On comparing both structures it is easily seen that a parallel shift of

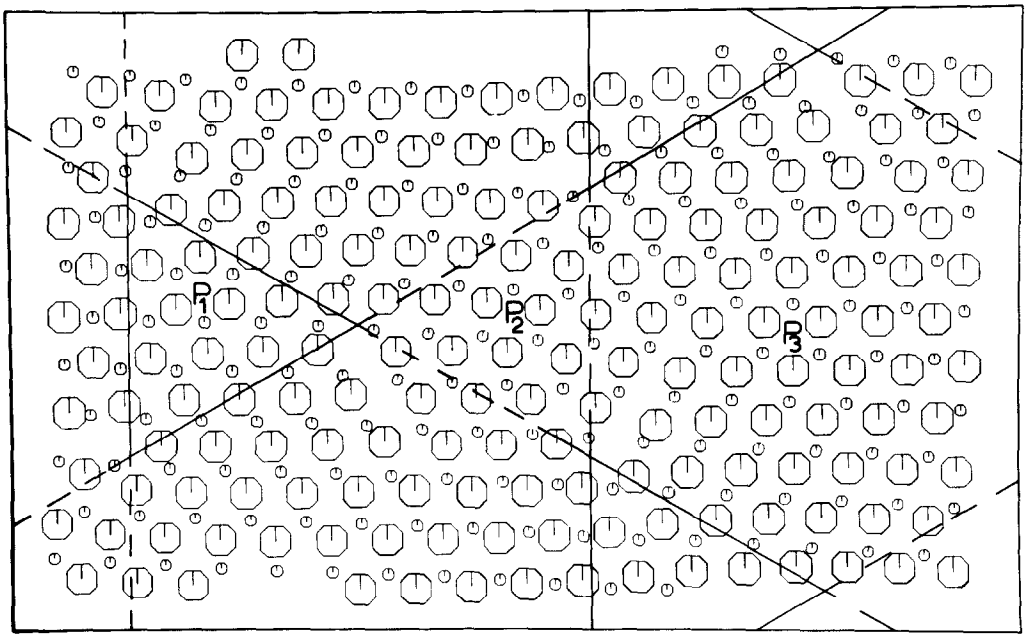

Fig. 6. Projected structure of the (111) planes $Z = -1$ and 0 from a $\Sigma = 91$ ($\theta = 53.99°$) twist boundary. The structure has the form of a six-star pattern.

the vertical dislocations in Fig. 6 over half the dislocation spacing transforms the configuration of Fig. 6 into the configuration of Fig. 5. As a result of such a shift to the left in Fig. 6, the dashed triangles in Fig. 6 disappear. This implies that the triangular structure of Fig. 5 consists entirely of single steps in the boundary. Apart from the six-star pattern observed in Fig. 2 there is evidence that in some areas the dislocation configuration is close to a triangular structure similar to that obtained in Fig. 5.

The relative stability of different configurations for a given boundary depends on the interatomic potential. Apart from the six-star pattern, the triangular structure was found, as depicted in Fig. 5. Using the pseudopotential for Al, this triangular structure appeared to have a lower internal energy than the six-star pattern structure for all the Σ boundaries under investigation. The internal energies of several boundary structures, triangular and six-star pattern, are plotted in Fig. 8. The various structures obtained for different coincidence orientations and interatomic potentials are summarized in Table 1. From this table it is seen that for a given twist boundary and interatomic potential two different structures can be obtained. If the cut-off of the interatomic potential is close to the second nearest neighbour the stacking fault energy is zero, and as a result even a third hexagonal pattern was found (Fig. 9). This configuration, however, is not relevant for twin boundary structures since it minimizes the stacking fault energy.

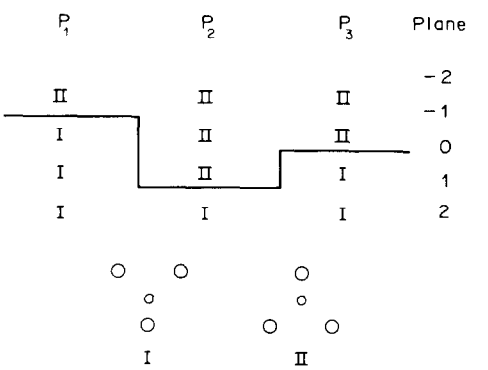

Fig. 7. Cross-section of the stacking of (111) planes in Fig. 6, along P_1P_3.

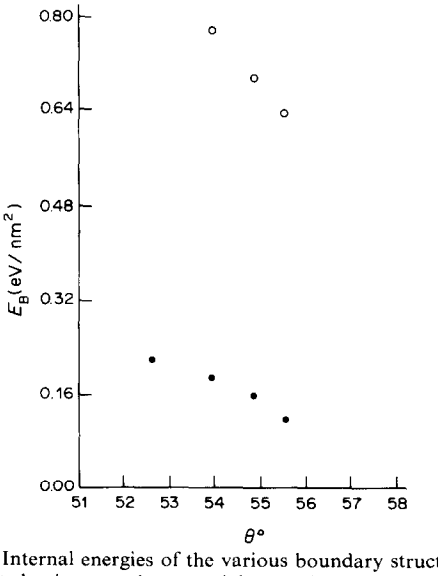

Fig. 8. Internal energies of the various boundary structures calculated using pseudo potential (●: triangular structure, ○: six—star pattern.)

Table 1

Σ	Rotation angle	Interatomic potential[a]	Computed structures[b]
169	55.59	DRT	S, T
		LJ	S, (T)[c]
127	54.91	DRT	S, T
		LJ	S, (T)[c]
91	53.99	DRT	S, T
		LJ	S, T
61	52.66	DRT	T
		LJ	T
37	50.57	DRT	T
		LJ	T

[a]DRT = Dagens-Rasolt-Taylor, cut-off = 1.00825 nm. LJ = Lennard–Jones, cut-off = 0.4824 nm.
[b]S, T represent a six-star and triangular pattern, respectively.
[c]Not explicitly calculated.

4. DISCUSSION AND CONCLUSIONS

Employing a pseudo-potential for Al in a numerical relaxation procedure for the configuration of near-coherent twin boundaries, two different structures have been generated. These structures can be described with the aid of a triangular and six-star pattern of Shockley partial dislocations as illustrated in Figs 5 and 6, respectively. It has been found that the computed energy of the triangular configuration is in general much lower than the energy of the six-star pattern as illustrated in Fig. 8. This may seem somewhat surprising, since inspection of Fig. 5 shows that the atoms in the neighbouring planes in the vicinity of the corners of the triangles are situated above each other. However, the energy difference between the two structures may be associated with the way in which the six-star pattern was generated. As described in the previous section, to obtain this pattern the central plane was divided among the two half crystals and this plane is still distorted after relaxation. Thus in the starting configuration the atoms *within* this plane are closer than in a well-ordered single crystal (111) plane, whereas the atoms lying on *adjacent* (111) planes are not much closer than the nearest neighbour distance in an f.c.c. lattice.

Experimentally a six-star pattern has been found in near-coherent twin boundaries in Au, as shown in Fig. 2 and also observed by Scott and Goodhew [9]. With regard to these observations two remarks should be made. First, the deviation from the exact twin misorientation is about ten times as small compared with the computed structures. Because of the limited size of the computer-simulated bicrystal it was not possible to obtain structures closer to the experimentally observed structures. Secondly, upon close inspection of Fig. 2 it may be observed that there are small regions in area C in which the network almost appears as a triangular structure, characterized by the absence of area of "white" contrast. This suggests that perhaps the energy difference in Au between both structures is not very large, as may have been anticipated from the previously discussed simple transformation of one structure into the other. This transformation preserves the dislocation density in the boundary plane. Also both structures consist of single atomic steps in the boundary, in contrast to a hexagonal or lozenge-shaped network which introduce double steps in the boundary, thereby increasing the boundary energy [9].

As a general conclusion of this work it appears satisfactory that experimentally observed structures in near-coherent twin boundaries in Au could be

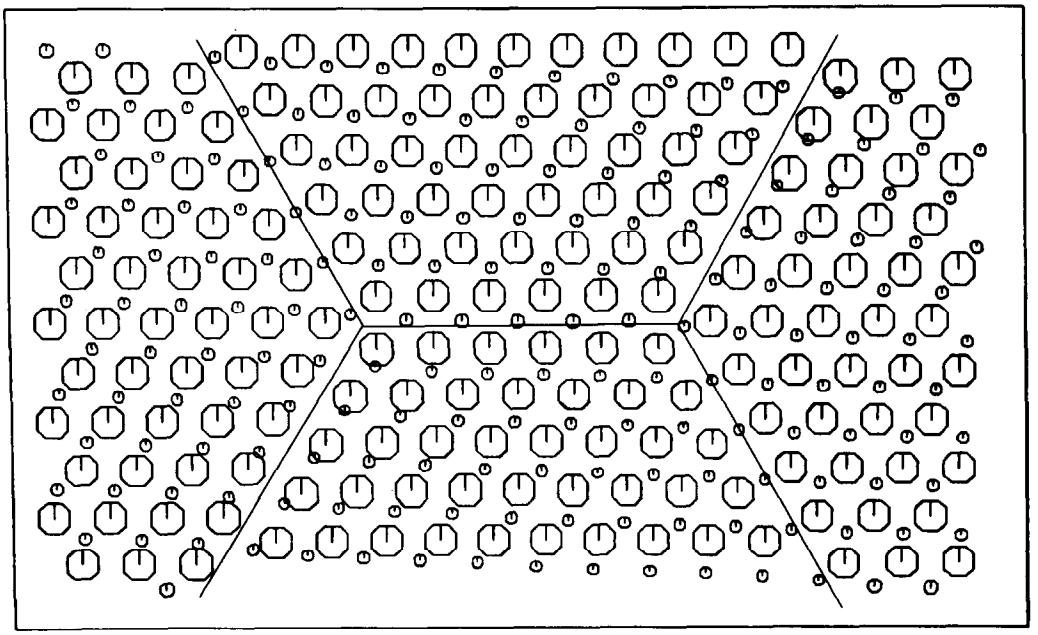

Fig. 9. Projected hexagonal structure of the (111) planes $Z = -1$ and 0 from a $\Sigma = 91$ ($\theta = 53.99°$) twist boundary.

reproduced in a computer simulation study based upon suitable potentials for Al. However, detailed agreement has not been obtained, the main discrepancy being the large energy difference between the triangular structure and the six-star pattern found in the simulations. Although the computed energy difference depicted in Fig. 8 tends to decrease with decreasing deviation from the twin orientation, it is not expected that the two structures have nearly the same energy close to 60°, as suggested by the experiments. Possible reasons for this behaviour are

(i) the inadequacy of the potentials for the description of defect structures in Au. Within the central-force potential approach possible volume expansion near the grain boundary has not been considered. From references [14, 15] can be concluded that in metals a central-force constant volume approach cannot be successful in predicting detailed structural properties of interfaces. The pair potential approach works as far as trends are concerned and does not work, for obvious reasons, in any detailed total energy calculation for a specific metallic system.

(ii) The inaccuracy of the calculation, e.g. the effect of fixed boundary conditions in the Z-direction on the atomic configurations calculated. To get more reliable results, a larger range of the potential should be used. An extension in the range of the potential forces us to increase the number of atoms in the simulated cell. This in turn leads to a decrease in the precision with which the configuration and therefore the energy of the grain boundary can be calculated [16].

Acknowledgements—This work is part of the research program of the Foundation for Fundamental Research on Matter (FOM, Utrecht) and has been made possible by financial support from the The Netherlands Organization for the Advancement of Pure Research (ZWO, The Hague).

REFERENCES

1. V. Vitek, A. P. Sutton, D. A. Smith and R. C. Pond, *Grain Boundary Structure and Kinetics*, p. 115. Am. Soc. Metals, Metals Part, Ohio (1980).
2. A. P. Sutton, *Int. Metals Rev.* **29,** 377 (1984).
3. A. Brokman, P. D. Bristowe and R. W. Balluffi, *Scripta metall.* **15,** 201 (1981).
4. H. J. Frost, M. F. Ashby and F. Spaepen, Techn. Rep. Division of Appl. Sci. Harvard Univ. (1982).
5. J. G. Erlings and F. W. Schapink, *Physica status solidi.* (a) **46,** 653 (1978).
6. J. J. C. Hamelink and F. W. Schapink, *Beitr. Elektr. Direktabb. Oberfl.* **16,** 213 (1983).
7. J. J. C. Hamelink and F. W. Schapink, *Phil. Mag.* **A44,** 1229 (1981).
8. W. T. Read, *Dislocations in Crystals.* McGraw-Hill, New York 1953.
9. R. F. Scott and P. J. Goodhew, *Phil. Mag.* **A44,** 873 (1981).
10. M. J. Weins, *Surf. Sci.* **31,** 138 (1972).
11. L. Dagens, M. Rasolt and R. Taylor, *Phys. Rev.* **B11,** 2726 (1975).
12. J. R. Heringa, J. Th. M. De Hosson and F. W. Schapink, *Scripta metall.* **17,** 1161 (1983).
13. J. Th. M. De Hosson, J. R. Heringa, F. W. Schapink, J. H. Evans and A. van Veen, *Surf. Sci.* **144,** 1 (1984).
14. J. Th. M. De Hosson, *Interatomic Potentials and Crystalline Defects* (edited by J. K. Lee), p. 3. Am. Inst. Min. Engrs, New York (1981).
15. J. Th. M. De Hosson, in *Handbook of Interatomic Potentials II, Metals* (edited by R. Taylor and M. Stoneham. Harwell (1982).
16. D. Wolf, *Acta metall.* **32,** 245 (1984).